

# AX-PET: Concept, Proof of Principle and First Results with Phantoms

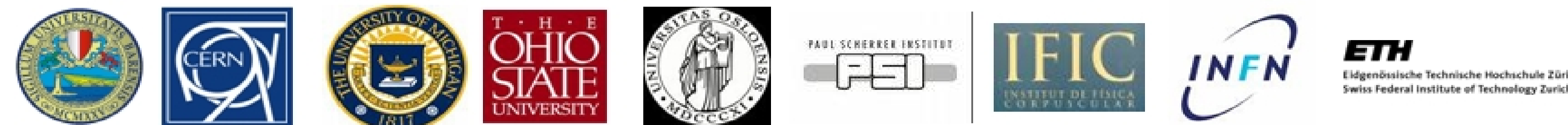


P. Solevi\*

University of Valencia – CSIC

On behalf of the AX-PET collaboration

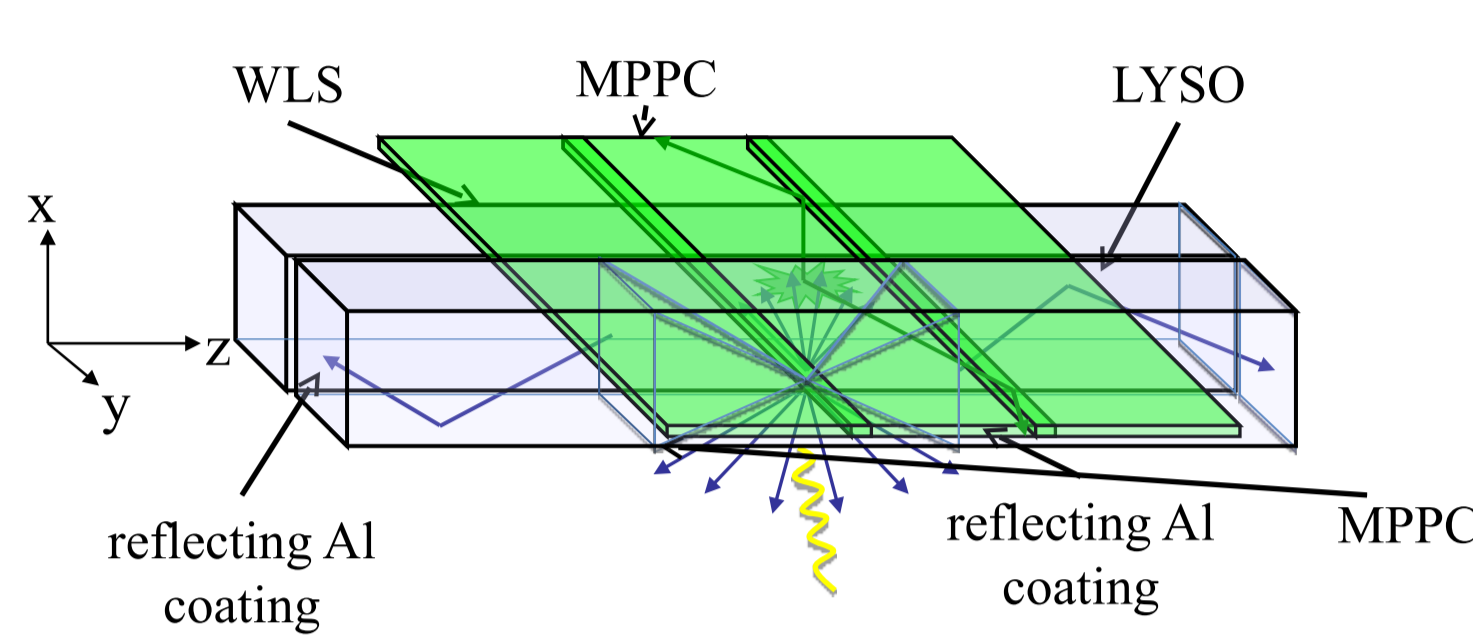
INFN Bari, Ohio State University, CERN, University of Michigan, University of Oslo, INFN Roma, University of Valencia, PSI Villigen, ETH Zurich



**Abstract:** AX-PET is a novel PET detector based on long axially arranged crystals and orthogonal Wavelength shifter (WLS) strips, both individually readout by Geiger-mode Avalanche Photo Diodes (G-APD). Its design was conceived in order to reduce the parallax error and simultaneously improve spatial resolution and sensitivity. Two modules set in coincidence were fully tested and characterized by means of point-like  $^{22}\text{Na}$  sources. AX-PET qualification measurements with  $^{18}\text{F}$  labeled FDG and PET phantoms mounted on a rotating gantry were realized, in order to explore its potential in more realistic acquisitions. AX-PET development and improvements are supported by dedicated Monte Carlo simulation, training platform for the reconstruction algorithms as well.

## 1. The AX-PET concept

- The crystals are axially arranged on different layers and provide the transverse coordinates  $x, y$
- Layers of wavelength shifter strips interleaved between the crystals yield the axial coordinate  $z$
- Full 3-D reconstruction of the impact point of the impinging 511 keV gammas
- Silicon Photo Multipliers individually readout both LYSO and WLS (combined PET/MRI possible)
- Potential to identify and reconstruct Compton events (Inter-Crystal Scatter) increasing the system sensitivity
- Spatial resolution independent on the depth of interaction
- Uncorrelated sensitivity and spatial resolution in the detector



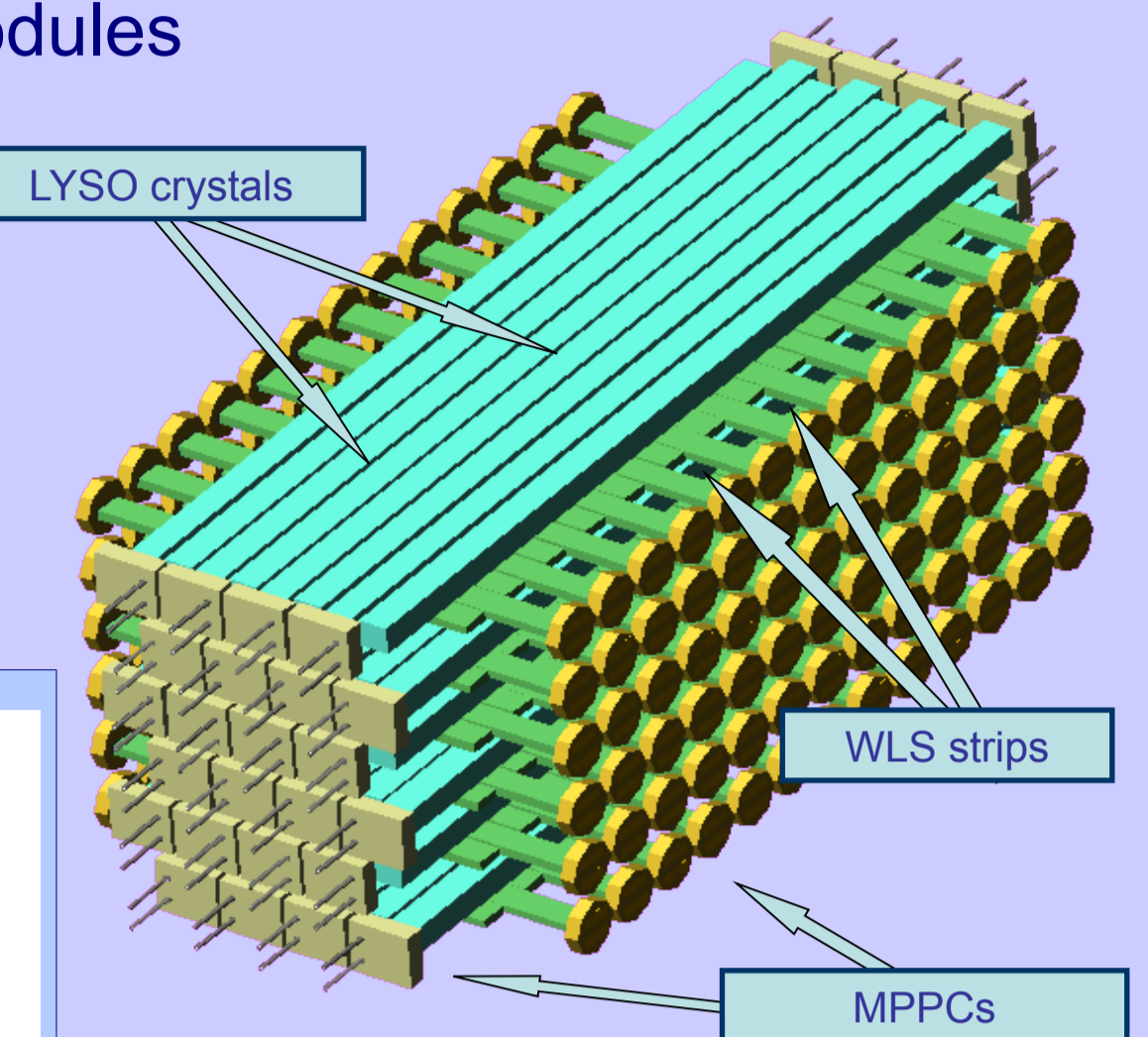
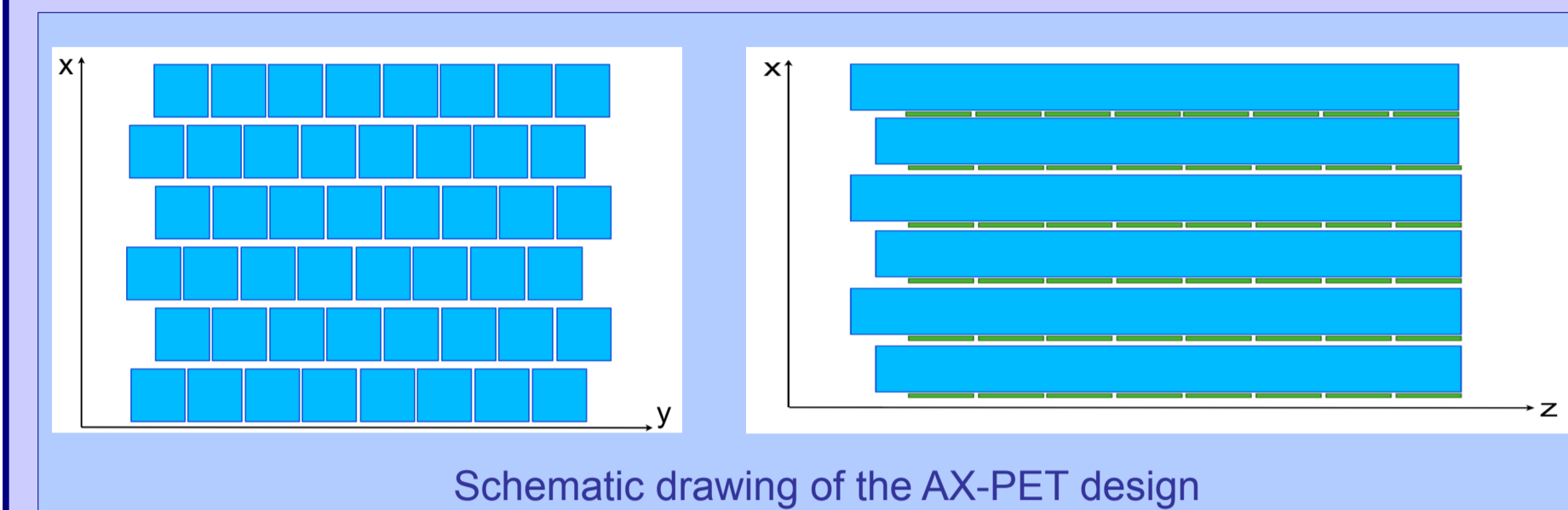
**The working principle**

- readout by MPPCs on one side
- reflective coating on opposite side
- photons inside cone of total reflection in LYSO detected by MPPC
- photons outside cone of total reflection in LYSO absorbed by WLS
- $x$  and  $y$  coordinates resolution determined by crystal section
- $z$  coordinate resolution improved by using the center of gravity method over a WLS cluster

## 2. Structure of the two modules

Six layers in each module

- Each layer composed of:
- 8 LYSO crystals in axial direction
  - 26 Wave Length Shifter (WLS) strips orthogonal to LYSOs
  - a thin carbon fiber plate to optically separate each layer



## 3. System components

### LYSO crystals

- Type: Saint-Gobain, PreLude™ 420 ( $\text{Lu}_{1.8}\text{Y}_{0.2}\text{SiO}_5:\text{Ce}$ )
- Dimensions:  $3 \times 3 \times 100 \text{ mm}^3$
- Light yield: 32 photons/keV
- Wavelength of peak emission spectrum: 420 nm
- Refractive index: 1.81 @ 420 nm
- Attenuation length @ 511 keV: 1.2 cm
- Effective light attenuation length: 42 cm
- Scintillation decay time: 42 ns, single exponential
- Density: 7.1 g/cm<sup>3</sup>

Picture of one fully assembled module (48 LYSOs + 156 WLS strips)

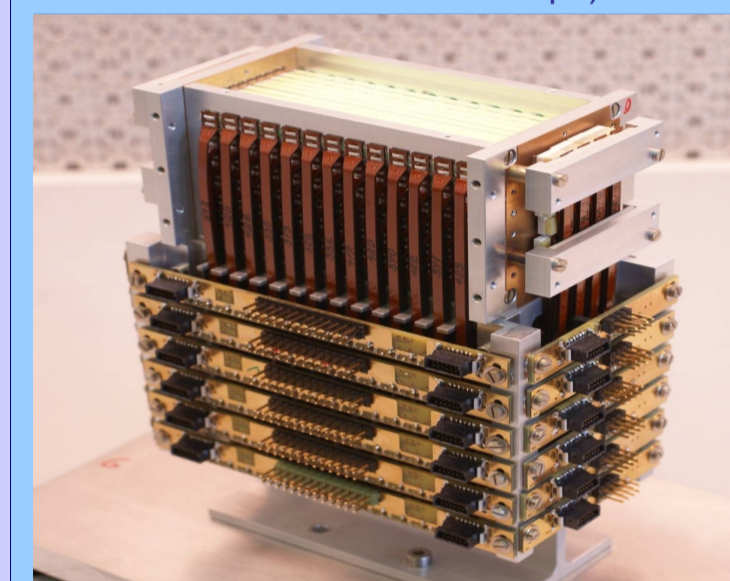


### Photo-detectors

- Type: Geiger-mode Avalanche Photo Diodes (G-APD)
- LYSO: Hamamatsu MPPC S10362-11-050C, 3600 cells
- WLS: Hamamatsu MPPC 3.22x1.19 OCTAGON-SMD, 782 cells

### Wave Length Shifting (WLS) strips

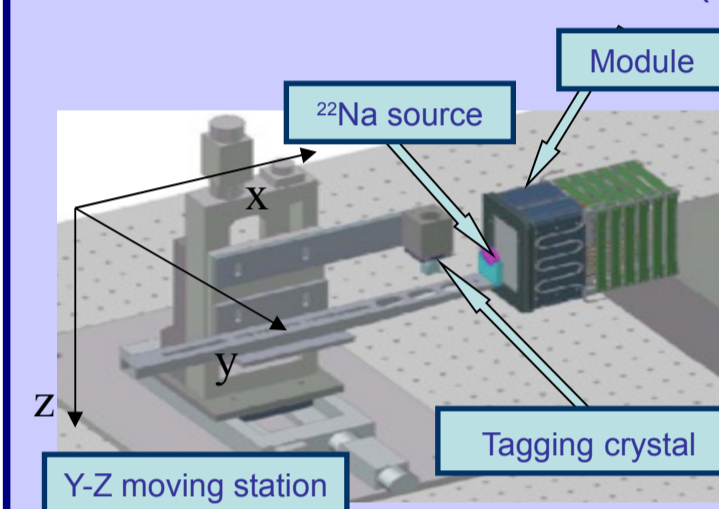
- Type: Eljen Technology EJ-280 (polyvinyltoluene)
- Dimensions:  $0.9 \times 3 \times 40 \text{ mm}^3$
- Quantum efficiency of the fluorescent dopant: 0.86
- Decay time: 8.5 ns
- Refractive index: 1.58
- Density: 1.023 g/cm<sup>3</sup>

### Readout electronics

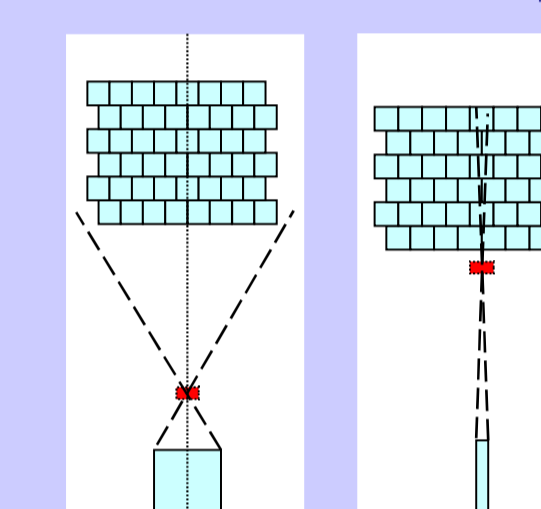
- signals from MPPCs fed into fast amplifiers (OPA846)
- signals from amplifiers fed into a charge integrating readout ASIC (VATAGP5, 128 channels), controlled by a VME DAQ system
- readout in sparse mode => channels above threshold only
- Self triggering or external trigger possible

## 4. Experimental setup for tests

In a first step the two modules have been individually characterized (left). Then the set-up was modified to perform coincidence measurements (right). Both measurements were performed with  $^{22}\text{Na}$  point sources.

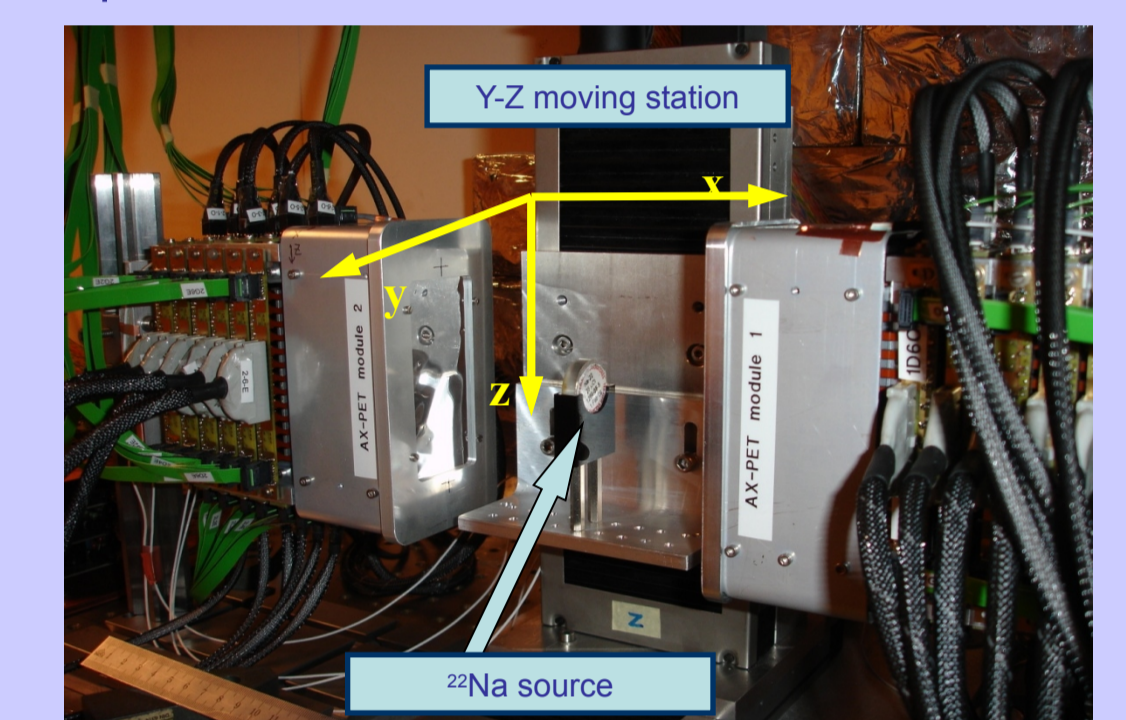


The source is placed between the module and the tagging crystal and can be moved to different positions. The source and the tagging crystal are mounted on a computer controlled moving station for precise positioning and scanning along  $y$  and  $z$  directions.



### Single module set-up

- Trigger signal: coincidence between energy sum of LYSO crystals of one module at the photopeak and tagging crystal
- Two LYSO tagging crystals of different dimensions:
  - "flat":  $2 \times 10 \times 12 \text{ mm}^3$  for broad illumination of the crystals (left picture)
  - "small":  $2 \times 2 \times 12 \text{ mm}^3$  for reduced spot size (right picture)



The two demonstrator modules in the AX-PET lab at CERN in the set-up used for coincidence measurements performed with a  $^{22}\text{Na}$  source (diameter: 250  $\mu\text{m}$ , activity: 925 kBq). Trigger signal: coincidence between the energy sums of the LYSO crystals of the two modules at the photopeak.

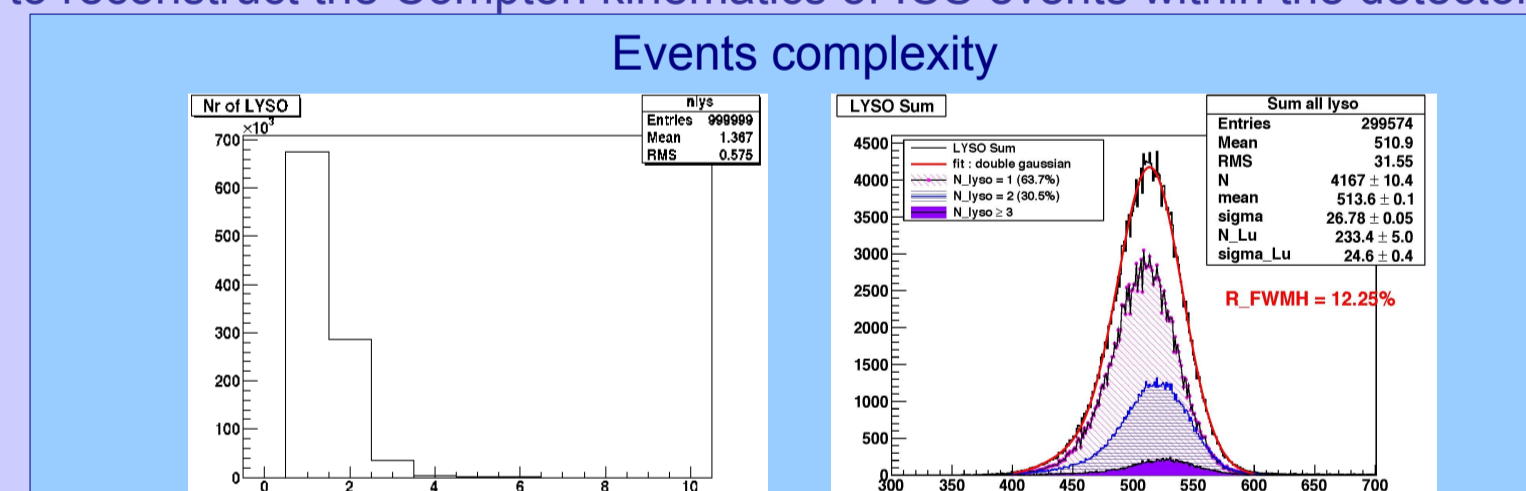
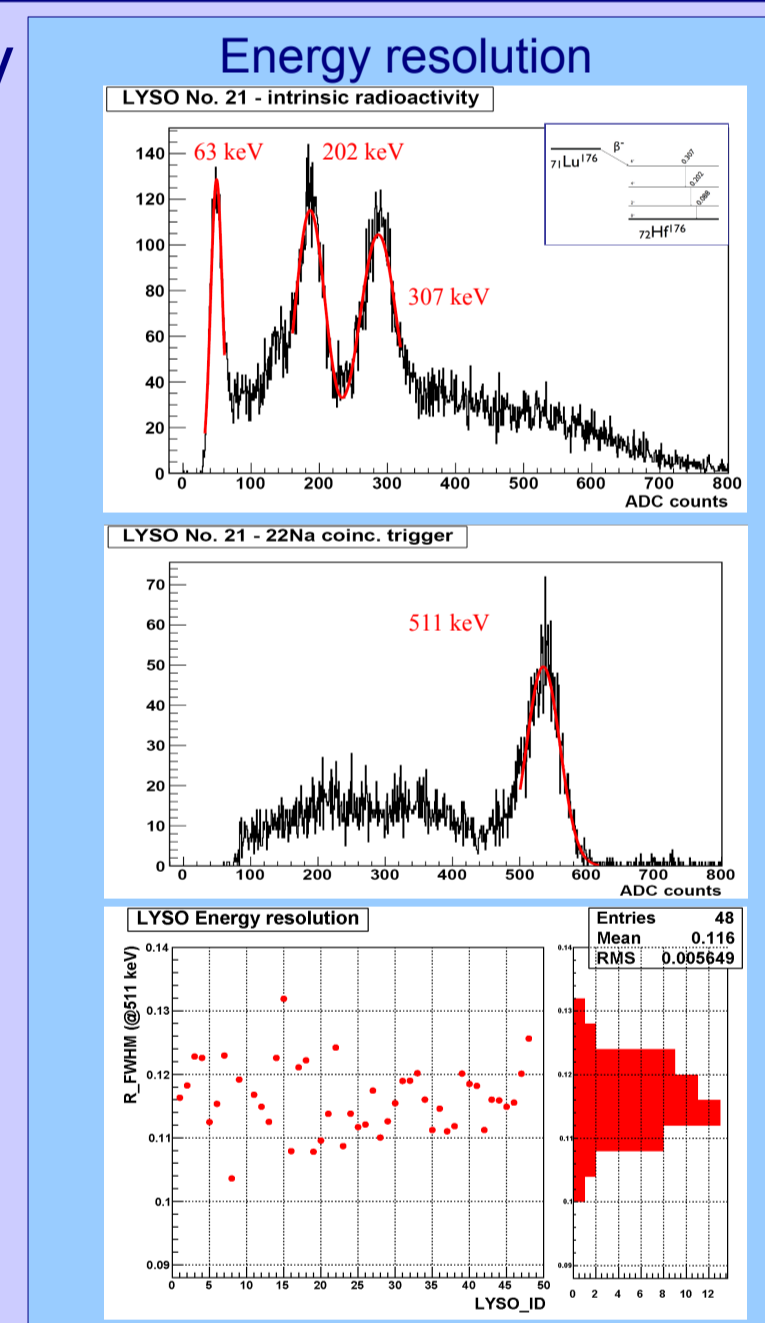
## 5. Energy resolution and events complexity

To calibrate the energy and to correct for the small non-linearity introduced by the MPPC saturation, we use two different data sets.

The first one (acquired in self-triggering mode), comprises two of the peaks of the  $^{176}\text{Lu}$  decay spectrum at 202 and 307 keV (natural radioactivity of LYSO) and the Lutetium  $K_{\alpha}$  escape line at 63 keV. The second one (acquired with the  $^{22}\text{Na}$  source), comprises the photoelectric peak at 511 keV. A log function is used to fit the three data points to take into account the saturation effect in the MPPCs.

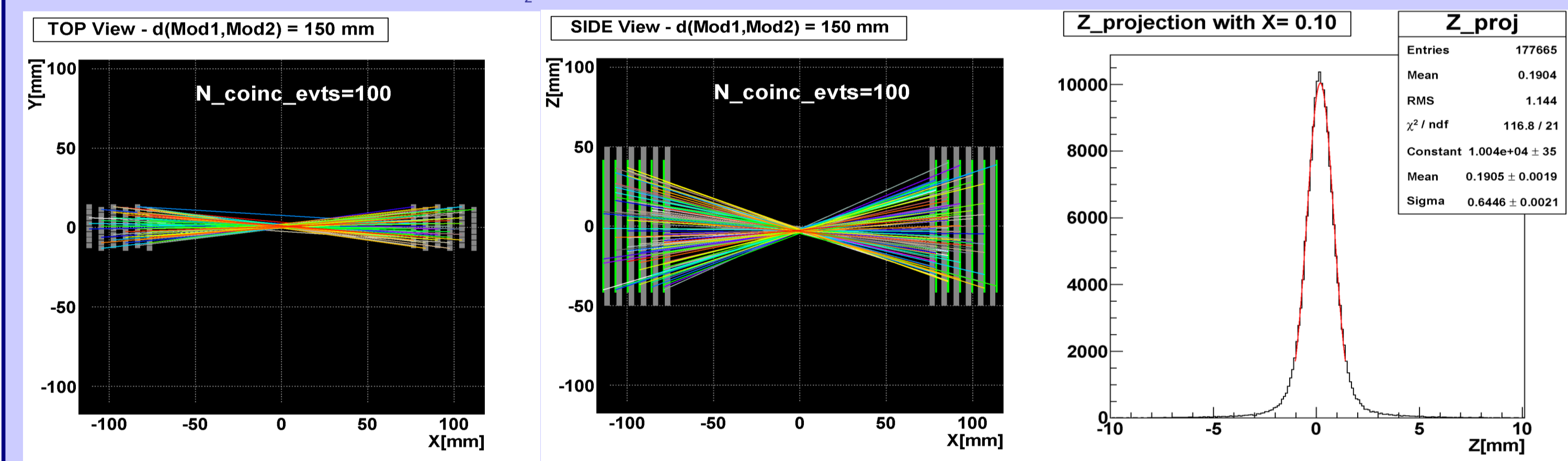
The average energy resolution of a crystal is 11.6% (FWHM) at 511 keV.

The measurements with point-like sources aim as well at exploring the events "morphology" e.g. the number of hit LYSO in order to quantify the amount of Inter-Crystal Scatter candidates. The good energy resolution of the device combined with the good spatial positioning capability makes feasible to reconstruct the Compton kinematics of ICS events within the detector.



## 6. First coincidence measurements and z resolution

Data was taken with the two modules at a distance of 150 mm and the  $^{22}\text{Na}$  point source placed in the middle, with a coincidence trigger. The colored lines are the connections between the detected  $(x, y, z)$ -positions of 511 keV photons in the two modules for the first 100 coincidence events. A top view (left) and a side view (middle figure) are shown. The right plot shows the intersection of these lines with a central plane at  $x = 0.1 \text{ mm}$ , position which minimizes the RMS of the distribution. The Gaussian fit indicates a resolution of  $\sigma_z = 0.64 \text{ mm}$  (1.51 mm FWHM).

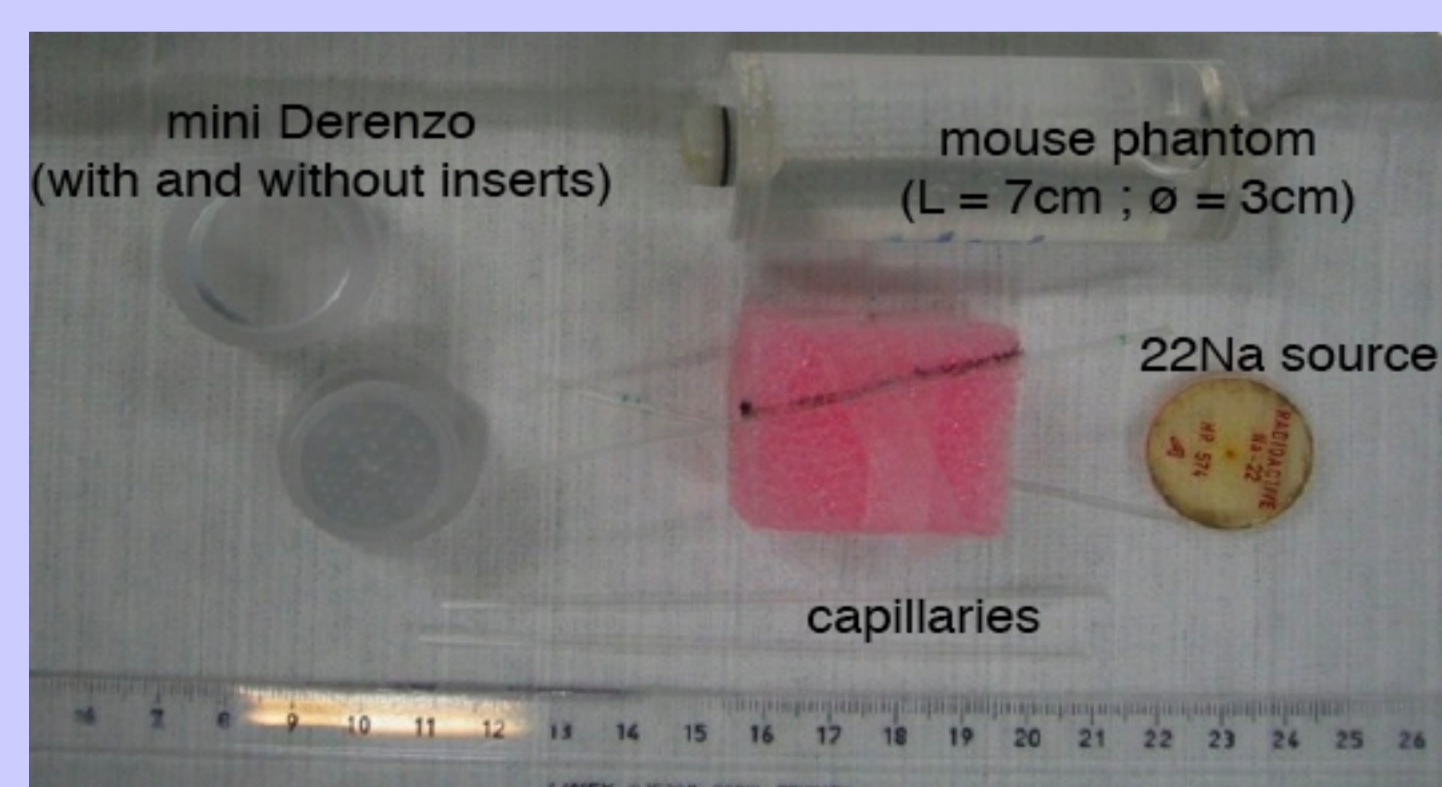


## 7. Measurements of extended sources

The two modules in coincidence were arranged on a portable station and a rotary table was placed in the centre, to position the source. AX-PET prototype was tested at the Institute of Pharmaceutical Sciences (ETHZ) by measuring different phantoms.

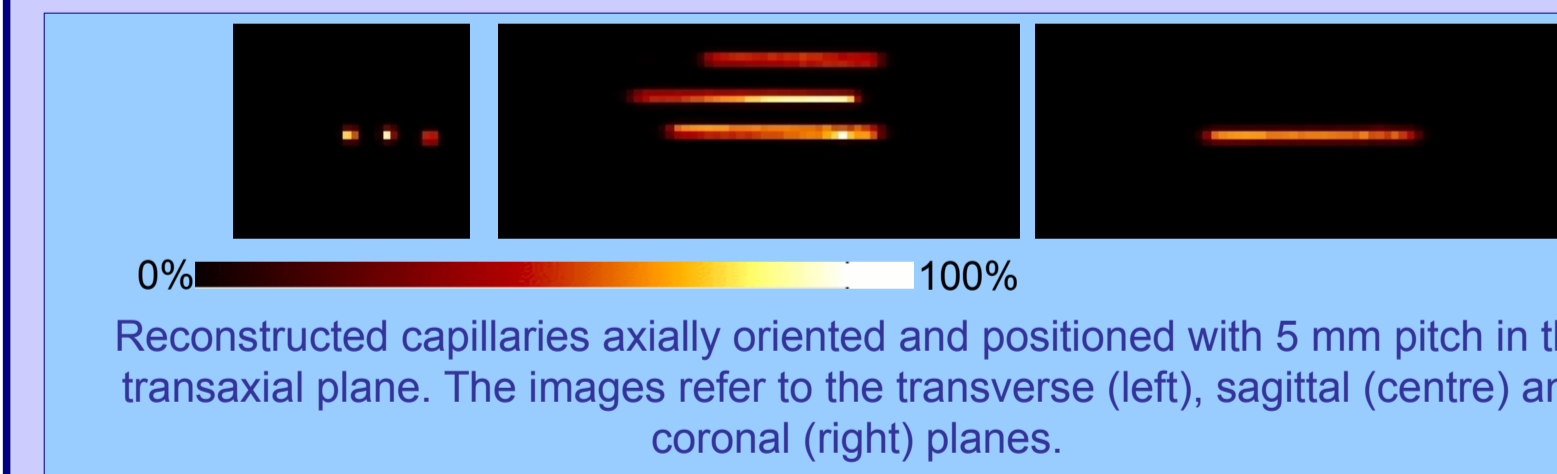
To assess the resolution capability of the scanner, a set of thin 3 cm long capillaries (1.4 mm inner diameter) and a micro-Derenzo were employed. To further investigate the image quality, a mouse-like phantom homogeneously filled with radioactive solution was measured. All phantoms were filled with various concentrations of  $^{18}\text{F}$ .

The phantoms were acquired by rotating the source support of 10 degrees step over  $\pi$  in order to cover the full extension of the sources.

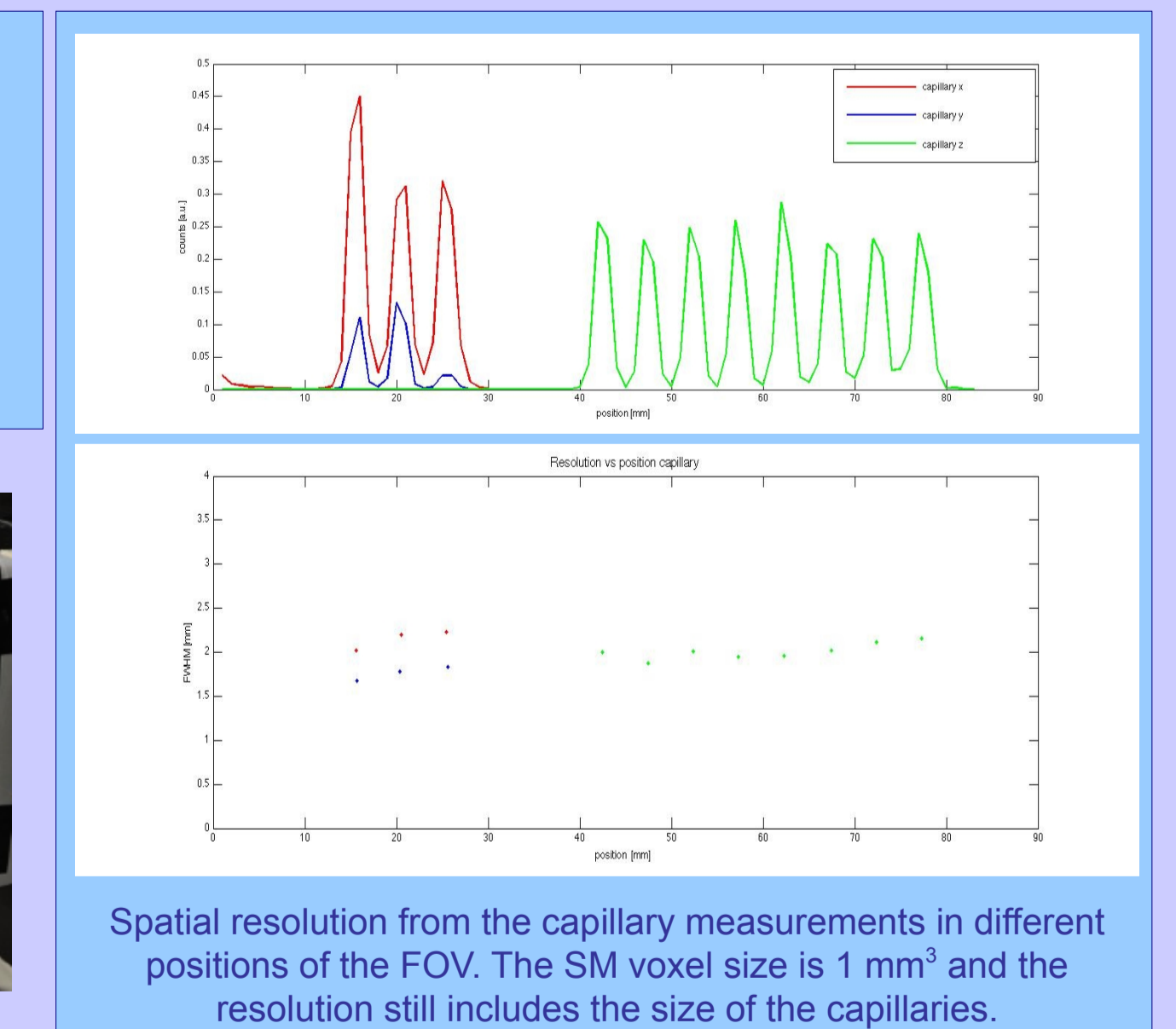
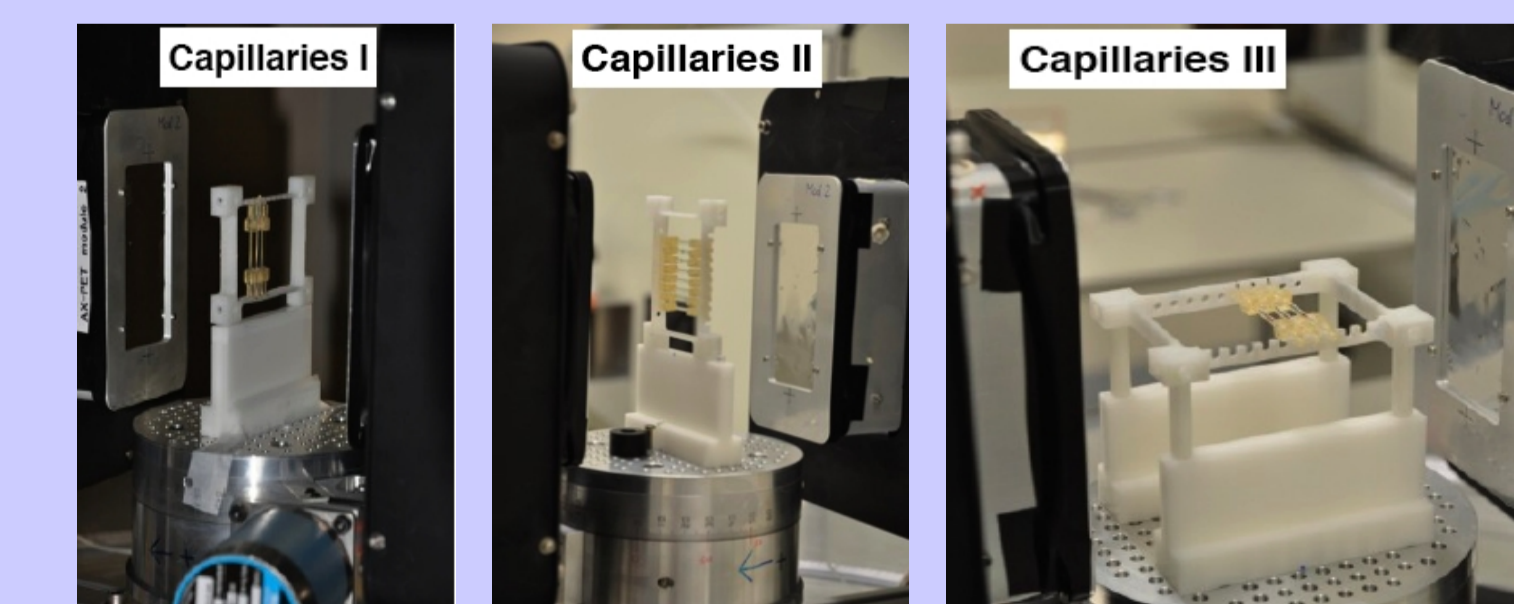


A dedicated image reconstruction software, based on Maximum-Likelihood Expectation Maximization (MLEM) was developed. The System Matrix has been computed using multi ray-tracing techniques. It models in detail the special geometry of the system and takes into account crystal attenuation and penetration effects (inner layers screen outer layers). The continuous axial coordinate is binned according to the WLS pitch. In the SM multi-ray tracing was used in order to take into account the finite size of the detection unit and reduce under-sampling artifacts in the final image.

## 8. Results



Reconstructed capillaries axially oriented and positioned with 5 mm pitch in the transaxial plane. The images refer to the transverse (left), sagittal (centre) and coronal (right) planes.



Spatial resolution from the capillary measurements in different positions of the FOV. The SM voxel size is  $1 \text{ mm}^3$  and the resolution still includes the size of the capillaries.

## 9. Conclusions and Outlook

- The tests carried out with point-like sources and extended phantoms successfully confirmed our expectations concerning the resolution of AX-PET and the tracking capability of the device.
- More features will be assessed in a second measurement campaign in which larger FOV will be scanned exploiting the possibility to change the relative angle of one module with respect to the other one.
- The measurements carried out pointed out the need of a better understanding of the count losses phenomena in the device that need to be corrected in order to achieve better images.
- The reconstruction still needs to be improved before any final performance assessment of AX-PET can be done:
  - the SM for the MLEM needs to include and exploit the  $z$  continuous information;
  - analytical reconstruction based on Filtered Back Projection (FBP) will be used soon to reconstruct the acquired phantoms;
  - dedicated algorithms for the recovery of ICS events have been tested on simulated data and will be applied soon to measured ones

### Acknowledgments

- This work is partially supported by the Marie Curie Intra-European Fellowship grant .
- The AX-PET collaboration would like to thanks ETH team?